Supporting Information for

Kinetic and Mechanistic Studies of the Formal (1+2)- and (1+4)-Cycloadditions of Germylenes to Conjugated Dienes

L. A. Huck and W. J. Leigh*

Synthesis and Characterization of Compounds S4

Figure S0. UV/vis absorption spectra of 3,4-dimethyl-1,1-diphenylgermacyclopent-3-ene (**1a**) and 3-methyl-1,1-diphenylgermacyclopent-3-ene (**4a**) in hexanes at 25 °C. S5

Steady-State Photolysis Experiments S6

Figure S1. Concentration *vs*. time plots from parallel photolyses of deoxygenated solutions of **1a** and **1e** (0.02 M) in C_6D_{12} containing MeOH (0.2 M). (a) **1a** and **1e**; slopes ($\times 10^2$): **1a** [□], -1.13 ± 0.02; **1e** [■], -1.23 ± 0.02. (b) Products; slopes ($\times 10^2$): **3a** [○], 0.97 ± 0.01; DMB from **1a** [●], 1.00 ± 0.01; **3e** [■], 1.09 ± 0.01; DMB from **1e** [□], 1.13 ± 0.01. S6

Figure S2. Product concentration vs. time plots from 254 nm photolysis of **1a** (0.032 M) in C_6D_{12} in the presence of isoprene (0.2 M): (slopes $\times 10^3$) DMB (●; 6.30 ± 0.36), **4a** (○; 5.25 ± 0.28), oligomers (■; 2.29 ± 0.22). S7

Figure S3. MALDI mass spectrum of the crude product mixture from photolysis of **1a** (0.02 M) in hexanes containing isoprene (0.3 M). S8

Table S1. Low-resolution mass spectral data of 1,1-diaryl-3-methylgermacyclopent-3-enes **4c,d,f** S8

Laser Flash Photolysis Experiments S9

Figure S4. Effects of added isoprene on the transient absorptions due to germylene **2b**: (a) raw transient decay profiles recorded at 500 nm in the presence of 0, 0.32, and 0.82 mM isoprene; and (b) the decay profiles from (a), after correction for the minor underlying contributions from digermene **5b**. The black lines in (b) are the non-linear least squares fits of the 0.32 and 0.82 mM data to two- and one-exponential decay equations, respectively. S9

Figure S5. Corrected 500 nm transient decay trace for $GePh_2$ in hexane containing 1.55 mM isoprene at 60°C, illustrating the procedure used for estimation of ΔA_{res} values. The solid red line is the fit of the data to two first-order exponential decays ($k_{decay} = k_{fast} + k_{slow}$) the fast component of which is due to reaction of the germylene with the diene. The black line is the value of ΔA_{res}, estimated as the break point in the bimodal decay. S9

Figure S6. Plots of (a) k_{decay} vs. [Q] and (b) ($\Delta A_o/\Delta A_{res,Q}$) vs. [Q], for the reaction of germylene **2a** with isoprene in deoxygenated hexanes at 25.0 °C. The solid lines are the linear least squares fits of the data to eq. 8 and 9, respectively. S10

Figure S7. Plots of (a) k_{decay} vs. [Q] and (b) ($\Delta A_o/\Delta A_{res,Q}$) vs. [Q], for the reaction of germylene **2c** with isoprene in deoxygenated hexanes at 25.0 °C. The solid lines are the linear least squares fits of the data to eq. 8 and 9, respectively. S10

Figure S8. Plots of (a) k_{decay} vs. [Q] and (b) ($\Delta A_o/\Delta A_{res,Q}$) vs. [Q], for the reaction of germylene **2d** with isoprene in deoxygenated hexanes at 25.0 °C. The solid lines are the linear least squares fits of the data to eq. 8 and 9, respectively. S11

Figure S9. Plots of (a) k_{decay} vs. [Q] and (b) ($\Delta A_o/\Delta A_{res,Q}$) vs. [Q], for the reaction of germylene **2e** with isoprene in deoxygenated hexanes at 25.0 °C. The solid lines are the linear least squares fits of the data to eq. 8 and 9, respectively. S11

Figure S10. Plots of (a) k_{decay} vs. [Q] and (b) ($\Delta A_o/\Delta A_{res,Q}$) vs. [Q], for the reaction of germylene **2f** with isoprene in deoxygenated hexanes at 25.0 °C. The solid lines are the linear least squares fits of the data to eq. 8 and 9, respectively. S12

Figure S11. Plots of (a) k_{decay} vs. [Q] and (b) ($\Delta A_o/\Delta A_{res,Q}$) vs. [Q], for the reaction of germylene **2g** with isoprene in deoxygenated hexanes at 25.0 °C. The solid lines are the linear least squares fits of the data to eq. 8 and 9, respectively. S12

Figure S12. Transient absorption spectra recorded by laser flash photolysis of 0.003 M solutions of (a) **1b** and (b) **1f** in deoxygenated hexanes containing 50 mM isoprene at 25 ^oC; the insets show decay profiles recorded at 290 nm along with the fits of the decays to first-order kinetics. The time windows after the laser pulse over which each spectrum was recorded are indicated. S13

Figure S13. Transient absorption spectra recorded by laser flash photolysis of a 0.003 M solution of **1g** in deoxygenated hexanes containing 50 mM isoprene at 25 °C – spectra were recorded 160-256 ns (○) and 1.12-1.184 μs (□) after the laser pulse. The inset shows the decay profile at 290 nm along with the fit of the decay to first-order kinetics. S13

Figure S14. Plots of ($\Delta A_0/\Delta A_{res,Q}$) vs. [isoprene], from laser photolysis of **1a, 1c,** and **1f** in deoxygenated hexanes over the temperature range of 13-65°C. The solid lines are the linear least squares fits of the data to eq. 11. S14

Figure S15. (a) Arrhenius and (b) van't Hoff plots for the reaction of diarylgermylenes **2c** and **2f** with isoprene in deoxygenated hexanes. S14

Figure S16. (a) Corrected decay profiles for germylene **2a** in deoxygenated hexanes containing 0, 3.0, 4.5, and 7.3 mM DMB, along with the non-linear least squares fits of the data to the sum of two exponential decays. (b) Transient absorption spectrum of vinylgermirane **7a** in deoxygenated hexanes containing 30 mM DMB at 25 °C; the inset shows the transient decay profile at 290 nm. (c) Plot of the residual germylene absorbance ratios, ($\Delta A_o/\Delta A_{res,Q}$) vs. [DMB]. S15

Table S2. Absolute rate and equilibrium constants for the reaction of **9a** (H), **9c** (Me) and **9f** (4-CF_3) with isoprene in dry, deoxygenated hexanes over the range of 13-62 °C. Errors are reported as ±2σ. All values are corrected for the density change of the solvent with temperature. S15

Table S3. Decay rates of the vinylgermirane **8a** at various temperatures, recorded in dry, deoxygentated hexanes in the presence of 50 mM isoprene. Corresponding K_{eq} (calculated from the van't Hoff parameters - see Figure 6b and Table 3) and k_2 values. Errors are reported as ±2σ. S16

Table S4. Arrhenius and van't Hoff parameters[a] for the reactions of germylenes **2a**, **2c**, and **2f** with isoprene in hexanes, calculated using the gas phase at 1 bar and 298.15K as standard state. S16

References S16

Synthesis and Characterization of Compounds

All synthetic preparations were carried out in flame-dried glassware under an atmosphere of dry nitrogen. Germacyclopentenes **1a**,[1] **1b**,[2] **1c**,**d**,**f**,[3] and **1g**[4] were prepared as previously described. ^{1}H NMR and ^{13}C NMR spectra were recorded on Bruker AV200 or AV600 spectrometers in $CDCl_3$ or C_6D_{12} (Cambridge Isotope Laboratories). High-resolution mass spectra were recorded on a Micromass TofSpec 2E mass spectrometer using electron impact ionization. MALDI mass spectra were recorded on a Waters/Micromass MALDI MicroMX mass spectrometer operating in reflectron mode (matrix: α-cyano-4-hydroxycinnamic acid). GC/MS analysis of product mixtures was performed using a Varian Saturn 2200 GC/MS/MS system equipped with a VF-5ms capillary column (30m×0.25mm; 0.25 μm; Varian, Inc.) using electron impact ionization. Static UV/vis absorption spectra were recorded on a Varian Cary 100 UV/vis spectrophotometer.

1,1-bis(3-fluorophenyl)-3,4-dimethyl-1-germacyclopentene (**1e**; mp 46.0-47.1°C) was prepared by an analogous method to the preparation of **1a**,[1] and purified via column chromatography (silica gel, hexanes) followed by multiple recrystallizations from hexanes. It was identified on the basis of the following spectroscopic data (*m/z* values marked with * indicate ions containing ^{74}Ge): ^{1}H NMR, δ = 1.86 (s, 6H, H_9), 2.09 (s, 4H, H_7), 7.05 (ddd, 2H, J = 8.6, 8.6, 2.7 Hz, H_4), 7.19 (dd, 2H, J = 8.4, 2.7 Hz, H_2), 7.26 (d, 2H, J = 7.2 Hz, H_6), 7.34 (ddd, 2H, J = 7.7, 7.7, 5.4 Hz, H_5). ^{13}C NMR, δ =19.48 (C_9), 25.53 (C_7), 116.10 (d, $^{2}J_{C\text{-}F}$ = 21 Hz, C_4), 120.69 (d, $^{2}J_{C\text{-}F}$ = 19 Hz, C_2), 129.83 (C_6), 130.04 (d, $^{3}J_{C\text{-}F}$ = 7 Hz, C_5), 130.84 (C_8), 140.64 (C_1), 162.88 (d, $^{1}J_{C\text{-}F}$ = 250 Hz, C_3). MS, m/z (intensity): 346.0* (40), 262.0* (25), 168.9* (25), 152.1 (100), 92.9 (30). HRMS: $C_{18}H_{18}F_2{}^{74}Ge$: calc.: 346.0588, found: 346.0574. Anal. calc. for $C_{18}H_{18}F_2Ge$, C 62.68, H 5.26; found, C 63.00, H

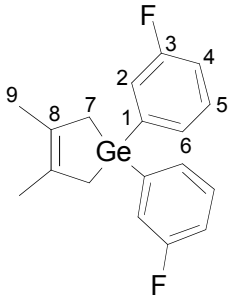

5.28. IR, cm^{-1} (intensity): 3062 (m), 2907 (m), 1598 (m), 1577 (m), 1475 (m), 1440 (w), 1416 (m), 1260 (m), 1211 (m), 1173 (w), 1161 (w), 1097 (m), 897 (m), 862 (m), 782 (m), 741 (m).

1,1-bis(3-fluorophenyl)-3-methyl-1-germacyclopentene (**4e**) was prepared in a manner analogous to that of **1e**, except that 1,1-dichloro-3-methyl-2,5-dihydro-1H-germole was used in place of 1,1-dichloro-3,4-dimethyl-2,5-dihydro-1H-germole. It was isolated as a pale yellow oil from the crude reaction mixture via silica column chromatography (hexanes) and identified based on the following spectroscopic data. ^{1}H NMR, δ = 1.86 (s, 3H, H_3), 1.89 (s, 2H, H_{10}), 2.00 (s, 2H, H_7), 5.63 (s, H, H_9), 7.06 (m, 2H, H_4), 7.19 (dd, 2H, H_2, J = 8.5, 2.6 Hz), 7.26 (m, 2H, H_6), 7.31 (m, 2H, H_5). ^{13}C NMR, δ = 19.16 (C_7), 22.54 (C_{11}), 22.66 (C_{10}), 116.19 (d, J = 21 Hz, C_4), 120.63 (d, J = 18 Hz, C_2), 125.18 (C_9), 129.75 (C_6), 130.10 (d, J = 7.5 Hz, C_5), 140.15 (C_8), 140.58 (C_1), 162.90 (d, J = 250 Hz, C_3). MS, m/z (intensity): 332.0* (52), 262.0* (40), 198.1* (20), 152.1 (100), 92.9* (38). HRMS: $C_{18}H_{18}F_2{}^{74}Ge$: calc.: 332.0432, found: 332.0437. IR, cm^{-1} (intensity): 3036 (m), 3004 (m), 2911 (br, m), 2060 (br, w), 1576 (s), 1475 (s), 1416 (s), 1260 (s), 1214 (s), 1161 (m), 1096 (s), 865 (s).

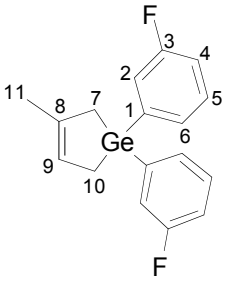

Figure S0. UV/vis absorption spectra of 3,4-dimethyl-1,1-diphenylgermacyclopent-3-ene (**1a**) and 3-methyl-1,1-diphenylgermacyclopent-3-ene (**4a**) in hexanes at 25 °C.

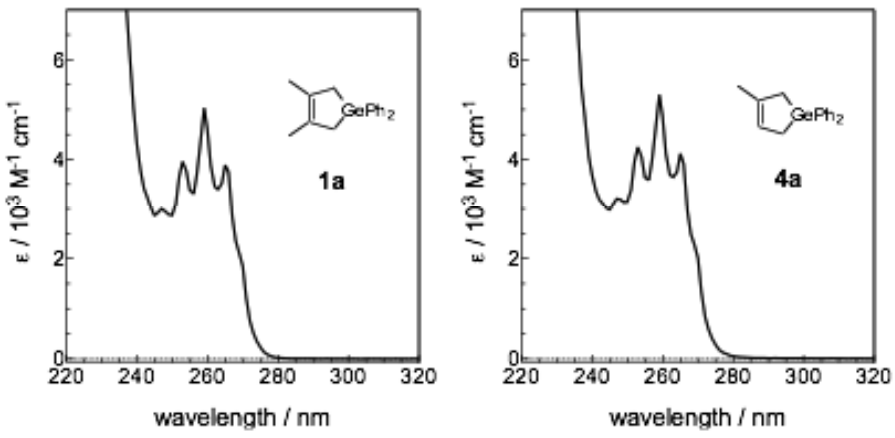

Steady state photolysis experiments.

(a) Quantum Yield Determination – Photolysis of **1e**

Solutions of **1a** and **1e** (0.02 M) in C_6D_{12} containing MeOH (0.2 M) were deoxygenated with a stream of dry argon and then irradiated in parallel, monitoring the course of the photolyses by ^{1}H NMR spectroscopy at 30 s intervals to ~10% conversion. DMB and the corresponding 1,1-diaryl-1-methoxygermane (**3a** and **3e**, respectively) were the only products detectable in the NMR spectra in both cases. Product yields were calculated (relative to consumed **1**) from therelative slopes of concentration vs. time plots (See Figure S1). The quantum yield for formation of **3e** from **1e** was calculated from the relative slopes of the plots for **3a** and **3e** and the value $\Phi_{3a} = 0.55 \pm 0.07$.[1]

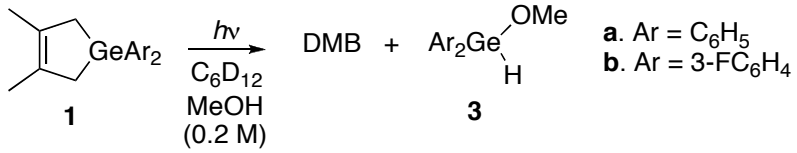

Diarylmethoxygermane **3e** was identified by comparison of its partial ^{1}H NMR spectrum to that of authentic **3a**:[1] δ = 3.56 (s, 3H, OC*H*$_3$), 6.11 (s, H, Ge*H*), 6.98-7.03 (m, 2H, Ar*H*). Unfortunately, the remaining aromatic proton resonances in its spectrum are obscured by those due to **1e**.

Figure S1. Concentration vs. time plots from parallel photolyses of deoxygenated solutions of **1a** and **1e** (0.02 M) in C_6D_{12} containing MeOH (0.2 M). (a) **1a** and **1e**; slopes (× 10^2): **1a** [□], -1.13 ± 0.02; **1e** [■], -1.23 ± 0.02. (b) Products; slopes (× 10^2): **3a** [○], 0.97 ± 0.01; DMB from **1a** [●], 1.00 ± 0.01; **3e** [■], 1.09 ± 0.01; DMB from **1e** [□], 1.13 ± 0.01.

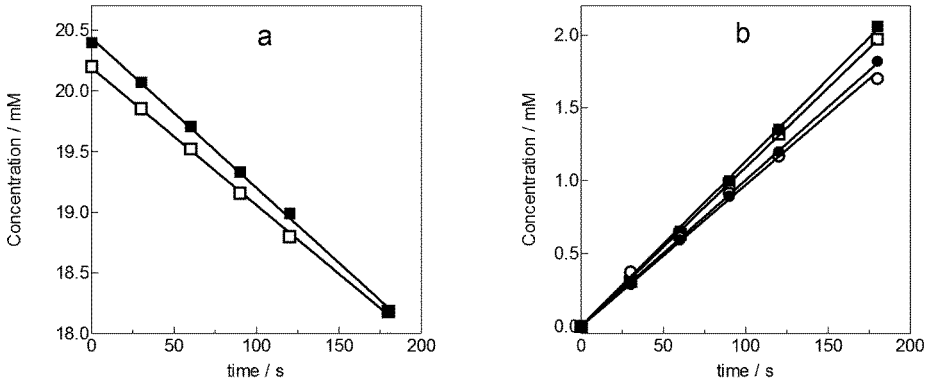

(b) Photolysis of **1a-f** in the presence of isoprene

A solution of **1a** (0.032 M) in C_6D_{12} containing isoprene (0.2 M) and Si_2Me_6 (*ca.* 2 mM) as internal integration standard was placed in a quartz NMR tube, purged briefly with dry argon and sealed. The sample was then irradiated in a Rayonet® photochemical reactor (Southern New England Ultraviolet Co.) equipped with a merry-go-round apparatus and 2 × RPR2537 (254 nm) lamps, and the progress of the reaction was monitored periodically by ^{1}H NMR spectroscopy (see Figure S1). Product concentrations were calculated from the following integrals (relative to Si_2Me_6 (δ 0.05; 18H)): DMB (δ 5.00; 2H and δ1.88; 6H – these values were averaged), **4a** (δ 5.71; 1H), $GePh_2$-containing oligomers (10H) were calculated by subtracting the integrals of the aromatic proton signals due to **1a** + **4a** (10H) from the total integral over δ 6.79-7.83. The relative chemical yields of the three products were then calculated from the relative slopes of the individual concentration vs. time plots (see Figure S2).

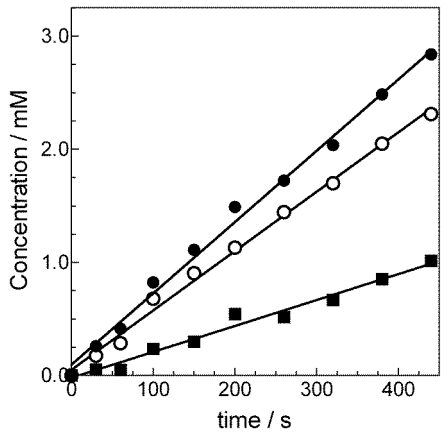

Figure S2. Product concentration *vs*. time plots from 254 nm photolysis of **1a** (0.032 M) in C_6D_{12} in the presence of isoprene (0.2 M): (slopes × 10^3) DMB (●; 6.30 ± 0.36), **4a** (○; 5.25 ± 0.28), oligomers (■; 2.29 ± 0.22).

A MALDI mass spectrum was recorded of the crude mixture from photolysis of **1a** (0.03 M) in deoxygenated hexanes containing 0.2 M isoprene for 7 minutes under conditions similar to those described above, and is shown in Figure S3. The major product detected exhibits a cluster of ions centered at m/z = 728.7, which is consistent with a molecule of formula $Ge_2Ph_4(C_5H_8)_4$ based on comparison of the isotopic distribution to the simulated spectrum.

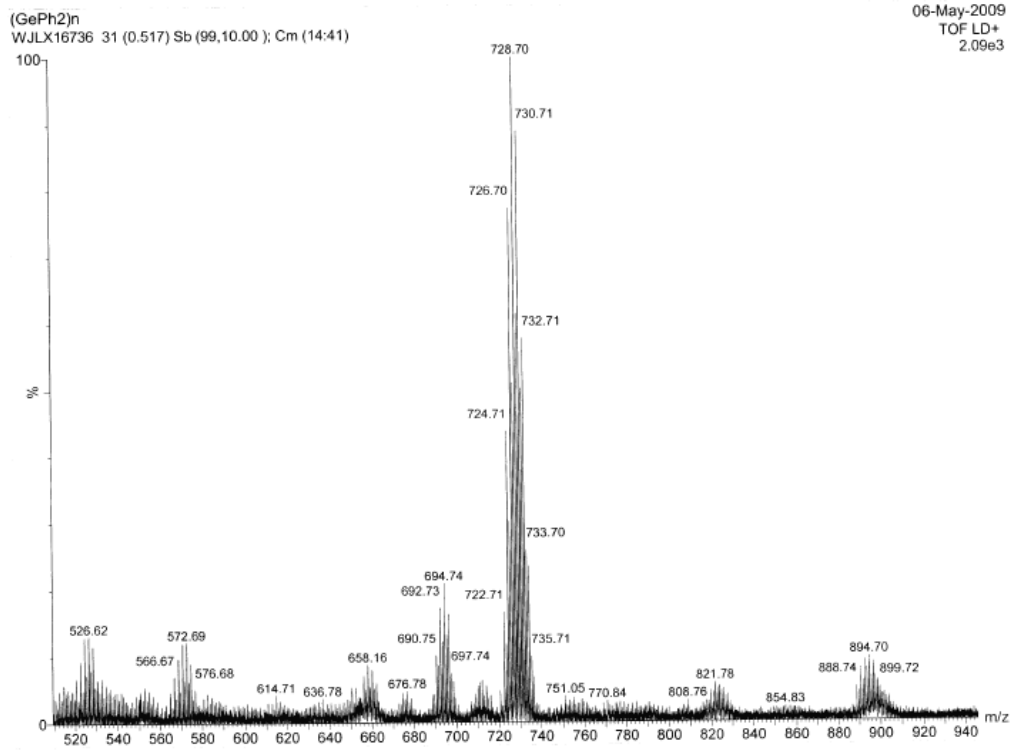

Figure S3. MALDI mass spectrum of the crude product mixture from photolysis of **1a** (0.02 M) in hexanes containing isoprene (0.3 M).

Deoxygenated solutions of **1b-g** (0.02 M) in hexanes containing isoprene (0.05 M) were irradiated as above (6 × 254 nm lamps; 20 minutes), and analyzed by GC/MS. In each case, the chromatogram showed evidence of only a single photolysis product, which eluted at a slightly shorter retention time compared to that of the starting compound. The products were identified as the corresponding 1,1-diaryl-3-methylgermacyclopent-3-enes **4b-g** based on their mass spectra (Table S1). The identity of **4b,e** in the photolysate from **1b,e** was further confirmed by spiking the mixture with an authentic sample.

Table S1. Low-resolution mass spectral data of 1,1-diaryl-3-methylgermacyclopent-3-enes **4c,d,f,g**.

4c	*p*-Me	324.2*(24), 256.3*(100), 181.5 (20), 165.2 (12).
4d	*p*-F	332.3*(70), 264.4*(100), 233.5*(12), 152.3 (35), 93.2*(35).
4f	*p*-CF_3	432.1*(52), 413.3* (12), 271.3 (85), 252.4 (100).
4g	*mm*-CF_3	568.3* (50), 549.7*(22), 389.3 (20), 388.6 (100).

[a] *m/z* values marked with * indicate ions containing ^{74}Ge

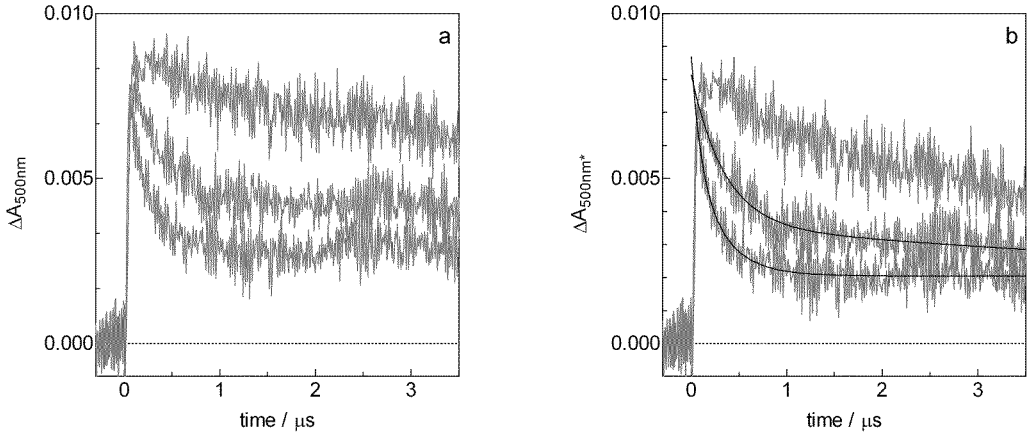

Figure S4. Effects of added isoprene on the transient absorptions due to germylene **2b**: (a) raw transient decay profiles recorded at 500 nm in the presence of 0, 0.32, and 0.82 mM isoprene; and (b) the decay profiles from (a), after correction for the minor underlying contributions from digermene **5b.** The black lines in (b) are the non-linear least squares fits of the 0.32 and 0.82 mM data to two- and one-exponential decay equations, respectively.

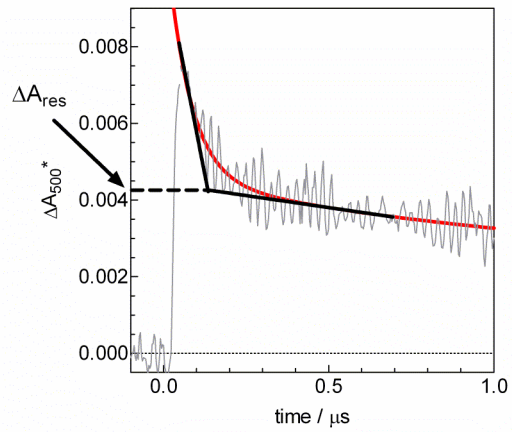

Figure S5. Corrected 500 nm transient decay trace for $GePh_2$ in hexane containing 1.55 mM isoprene at 60°C, illustrating the procedure used for estimation of ΔA_{res} values. The solid red line is the fit of the data to two first-order exponential decays ($k_{decay} = k_{fast} + k_{slow}$) the fast component of which is due to reaction of the germylene with the diene. The black line is the value of ΔA_{res}, estimated as the break point in the bimodal decay.

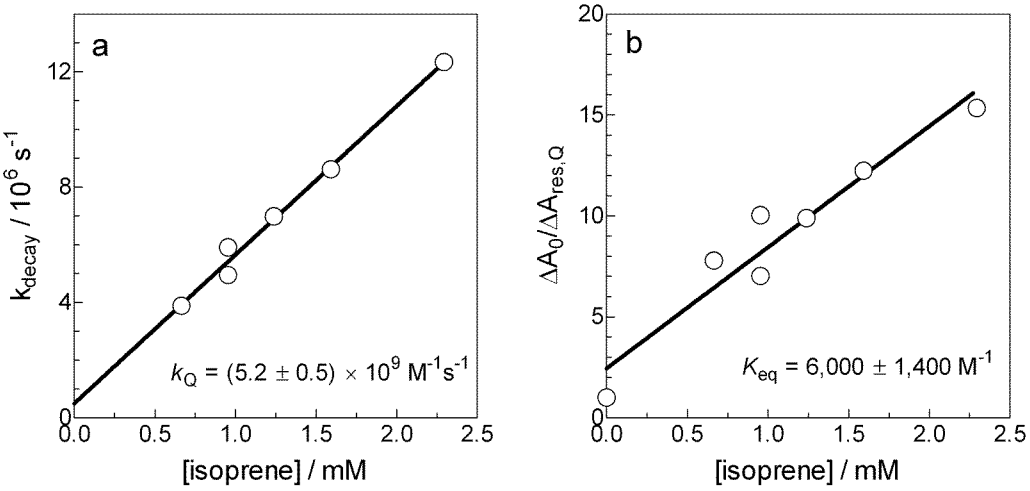

Figure S6. Plots of (a) k_{decay} vs. [Q] and (b) ($\Delta A_o/\Delta A_{res,Q}$) vs. [Q], for the reaction of germylene **2a** with isoprene in deoxygenated hexanes at 25.0 °C. The solid lines are the linear least squares fits of the data to eq. 8 and 9, respectively.

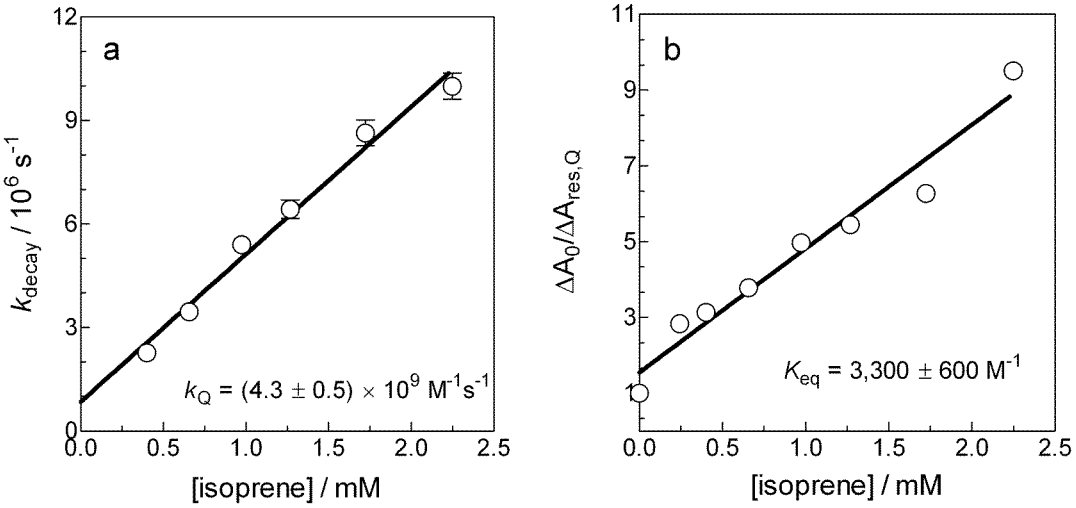

Figure S7. Plots of (a) k_{decay} vs. [Q] and (b) ($\Delta A_o/\Delta A_{res,Q}$) vs. [Q], for the reaction of germylene **2c** with isoprene in deoxygenated hexanes at 25.0 °C. The solid lines are the linear least squares fits of the data to eq. 8 and 9, respectively.

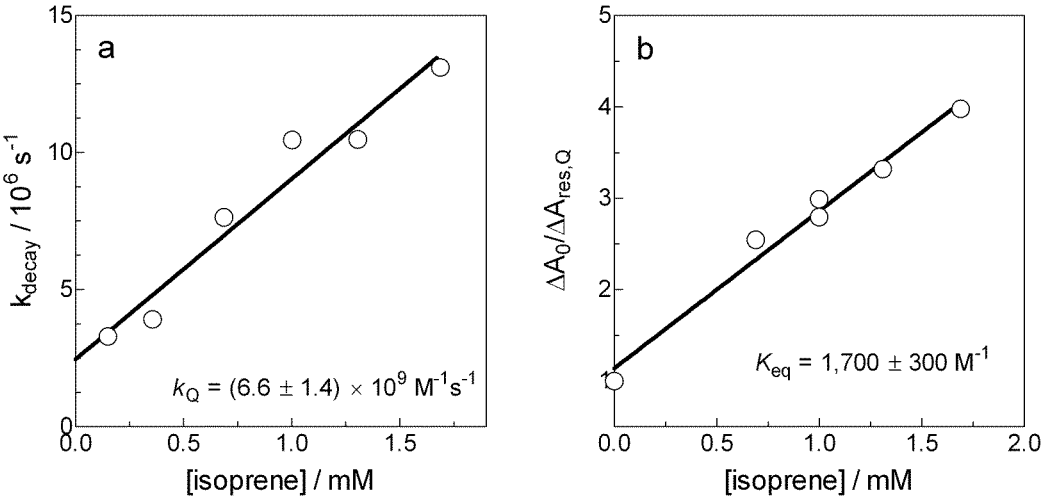

Figure S8. Plots of (a) k_{decay} vs. [Q] and (b) ($\Delta A_o/\Delta A_{res,Q}$) vs. [Q], for the reaction of germylene **2d** with isoprene in deoxygenated hexanes at 25.0 °C. The solid lines are the linear least squares fits of the data to eq. 8 and 9, respectively.

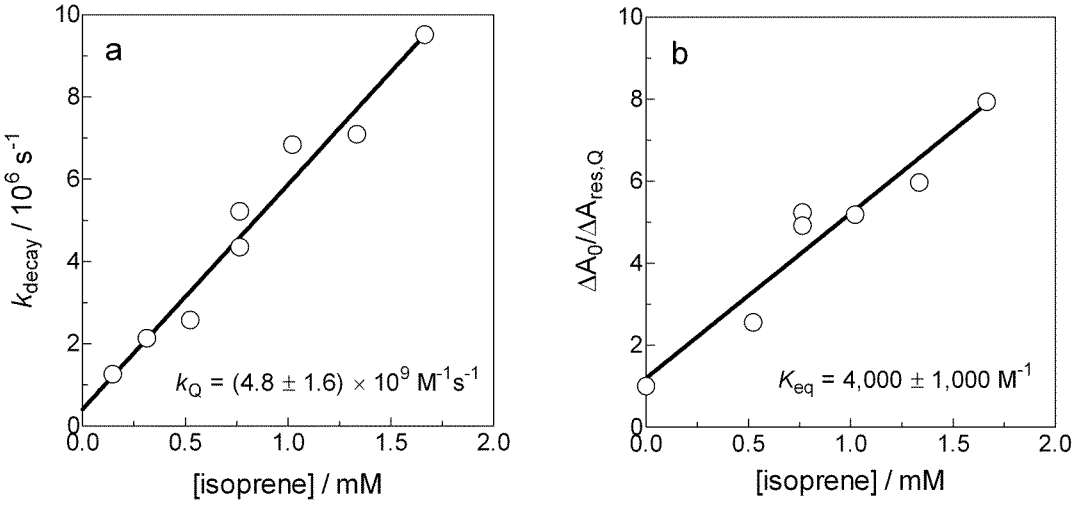

Figure S9. Plots of (a) k_{decay} vs. [Q] and (b) ($\Delta A_o/\Delta A_{res,Q}$) vs. [Q], for the reaction of germylene **2e** with isoprene in deoxygenated hexanes at 25.0 °C. The solid lines are the linear least squares fits of the data to eq. 8 and 9, respectively.

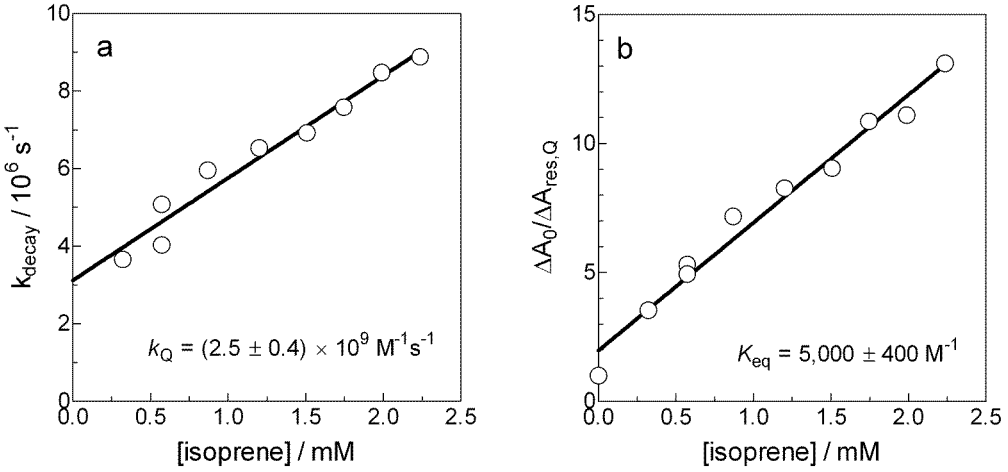

Figure S10. Plots of (a) k_{decay} vs. [Q] and (b) ($\Delta A_o/\Delta A_{res,Q}$) vs. [Q], for the reaction of germylene **2f** with isoprene in deoxygenated hexanes at 25.0 °C. The solid lines are the linear least squares fits of the data to eq. 8 and 9, respectively.

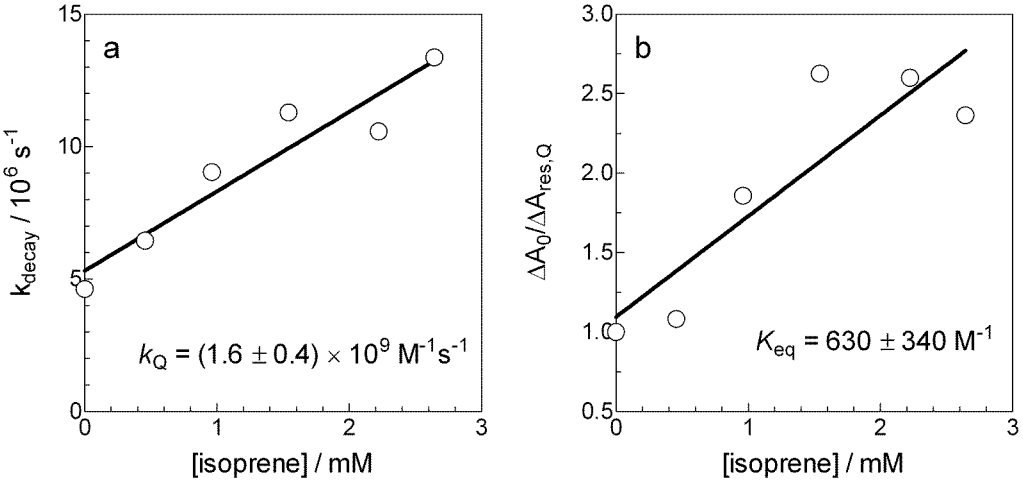

Figure S11. Plots of (a) k_{decay} vs. [Q] and (b) ($\Delta A_o/\Delta A_{res,Q}$) vs. [Q], for the reaction of germylene **2g** with isoprene in deoxygenated hexanes at 25.0 °C. The solid lines are the linear least squares fits of the data to eq. 8 and 9, respectively.

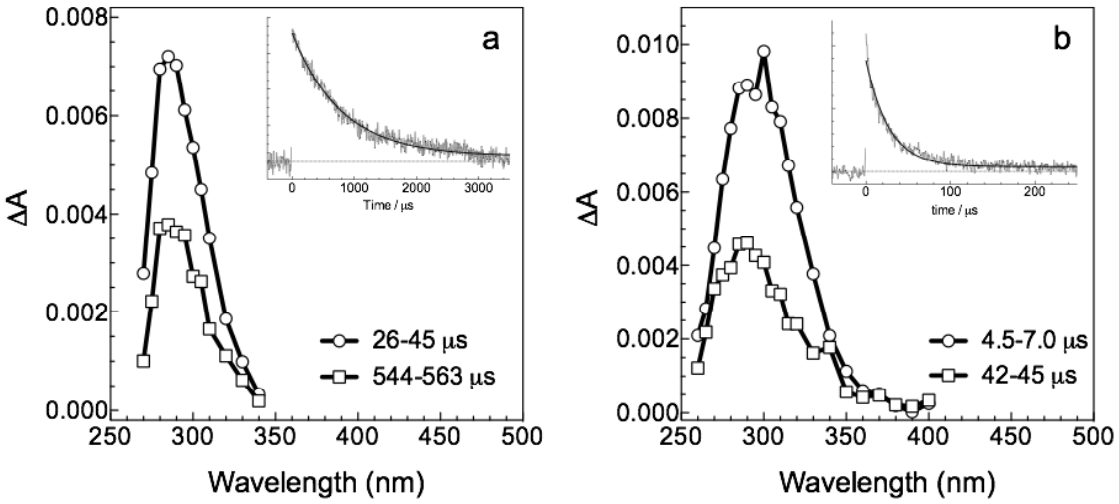

Figure S12. Transient absorption spectra recorded by laser flash photolysis of 0.003 M solutions of (a) **1b** and (b) **1f** in deoxygenated hexanes containing 50 mM isoprene at 25 °C; the insets show decay profiles recorded at 290 nm along with the fits of the decays to first-order kinetics. The time windows after the laser pulse over which each spectrum was recorded are indicated.

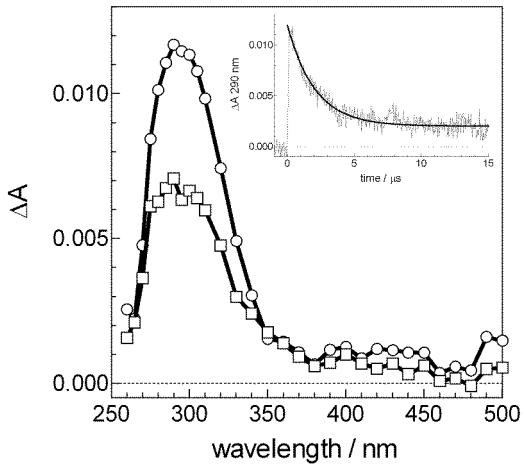

Figure S13. Transient absorption spectra recorded by laser flash photolysis of a 0.003 M solution of **1g** in deoxygenated hexanes containing 50 mM isoprene at 25 °C – spectra were recorded 160-256 ns (○) and 1.12-1.184 μs (□) after the laser pulse. The inset shows the decay profile at 290 nm along with the fit of the decay to first-order kinetics.

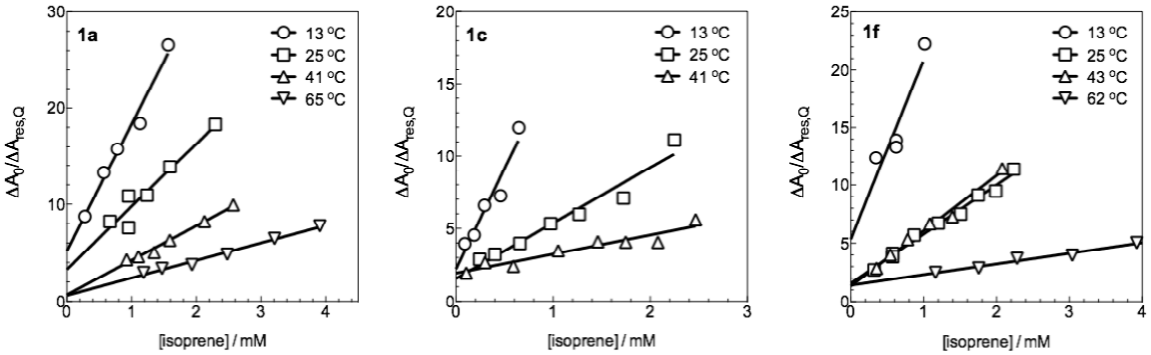

Figure S14. Plots of ($\Delta A_0/\Delta A_{res,Q}$) vs. [isoprene], from laser photolysis of **1a, 1c,** and **1f** in deoxygenated hexanes over the temperature range of 13-65°C. The solid lines are the linear least squares fits of the data to eq. 11.

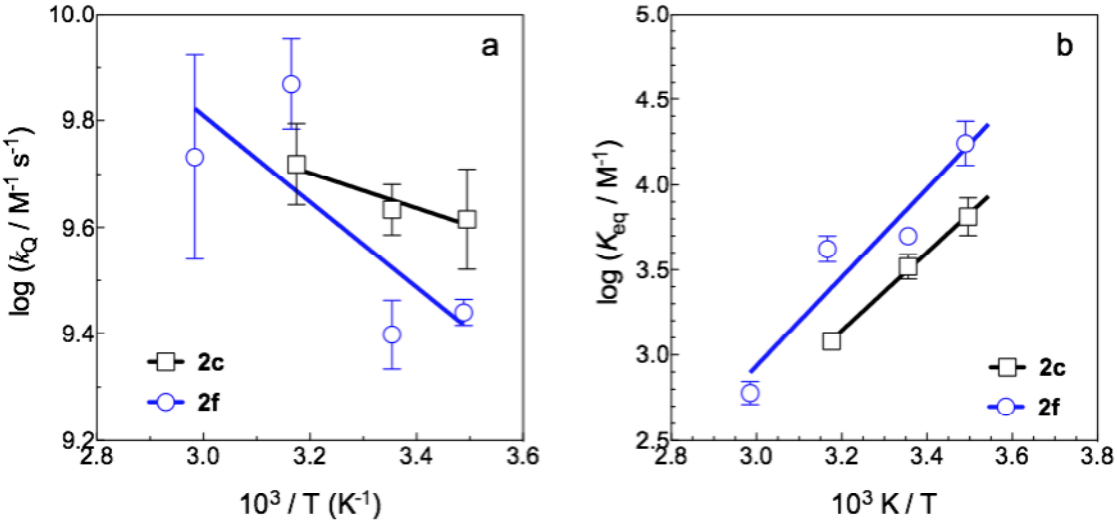

Figure S15. (a) Arrhenius and (b) van't Hoff plots for the reaction of diarylgermylenes **2c** and **2f** with isoprene in deoxygenated hexanes.

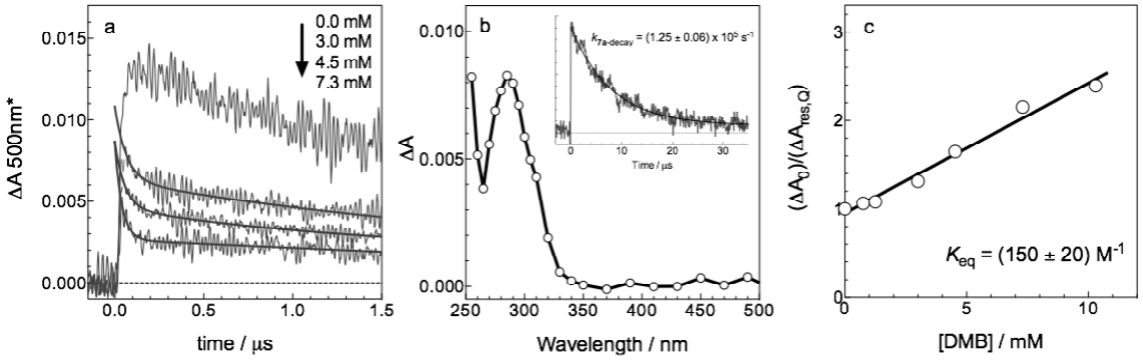

Figure S16. (a) Corrected decay profiles for germylene **2a** in deoxygenated hexanes containing 0, 3.0, 4.5, and 7.3 mM DMB, along with the non-linear least squares fits of the data to the sum of two exponential decays. (b) Transient absorption spectrum of vinylgermirane **7a** in deoxygenated hexanes containing 30 mM DMB at 25 °C; the inset shows the transient decay profile at 290 nm. (c) Plot of the residual germylene absorbance ratios, ($\Delta A_o/\Delta A_{res,Q}$) vs. [DMB].

Table S2. Absolute rate and equilibrium constants for the reactions of germylenes **2a** (H), **2c** (Me) and **2f** (4-CF_3) with isoprene in deoxygenated hexanes over the range of 13-62 °C. Errors are reported as ±2σ. All values are corrected for the density change of the solvent with temperature.

T / °C	k_Q / 10^9 M^{-1}s^{-1}	K_{eq} / 10^3 M^{-1}
	2a	
14.3	3.8 ± 0.5	13.2 ± 3.0
25.0	5.2 ± 0.5	6.0 ± 1.5
40.5	4.7 ± 0.4	2.8 ± 0.2
61.0	3.3 ± 1.2	1.2 ± 0.1
	2c	
13.0	4.1 ± 1.0	6.5 ± 1.9
25.0	4.3 ± 0.5	3.3 ± 0.6
41.8	5.2 ± 1.0	1.2 ± 0.4
	2f	
13.5	2.8 ± 1.6	17.5 ± 6.0
25.0	2.5 ± 0.4	5.0 ± 0.5
45.7	9.3 ± 2.4	4.2 ± 0.8
62.0	5.4 ± 3.0	0.6 ± 0.1

Table S3. Decay rates of the vinylgermirane **6a** at various temperatures, recorded in dry, deoxygentated hexanes in the presence of 50 mM isoprene. Corresponding K_{eq} (calculated from the van't Hoff parameters - see Figure 4 and Table 2) and $k_{(1+4)}$ values. Errors are reported as ±2σ.

Temp / °C	$k_{\mathbf{6a}\text{-decay}}$ / 10^3 s^{-1}	K_{eq} / 10^3 M^{-1}	$k_{(1+4)}$ / 10^7 M^{-1} s^{-1}
10.6	0.806 ± 0.018	14.9 ± 1.2	1.20 ± 0.09
14.3	1.11 ± 0.03	12.0 ± 1.0	1.33 ± 0.11
19.3	1.75 ± 0.04	9.0 ± 0.72	1.57 ± 0.13
25.5	2.20 ± 0.07	6.34 ± 0.51	1.39 ± 0.12
34.1	3.85 ± 0.19	4.03 ± 0.32	1.55 ± 0.13
34.5	4.17 ± 0.15	3.94 ± 0.32	1.65 ± 0.13
38.2	5.38 ± 0.27	3.27 ± 0.26	1.76 ± 0.14
43.5	7.25 ± 0.43	2.52 ± 0.20	1.83 ± 0.15
43.9	8.46 ± 0.52	2.47 ± 0.20	2.09 ± 0.17
49.9	10.5 ± 0.60	1.86 ± 0.15	1.94 ± 0.16
52.0	12.1 ± 1.00	1.69 ± 0.14	2.04 ± 0.17

Table S4. Arrhenius and van't Hoff parameters[a] for the reactions of germylenes **2a**, **2c**, and **2f** with isoprene in hexanes, calculated using the gas phase at 1 bar and 298.15K as standard state.[a]

	2a (H)	**2c** (4-Me)	**2f** (4-CF_3)
E_a / kcal mol^{-1}	-1.4 ± 2.5	+0.9 ± 0.8	+3.4 ± 5.2
log (A / bar^{-1})	+7 ± 2	+9 ± 1	+11 ± 4
ΔG / kcal mol^{-1}	-3.3 ± 0.1	-2.9 ± 0.1	-3.1 ± 0.2
ΔH / kcal mol^{-1}	-10.3 ± 1.1	-11.1 ± 0.9	-12 ± 6
ΔS / cal K^{-1} mol^{-1}	-23 ± 4	-28 ± 3	-29 ± 20

a. errors are quoted as ±2σ.

References

1. Leigh, W. J.; Harrington, C. R.; Vargas-Baca, I., *J. Am. Chem. Soc.* **2004**, *126*, 16105.
2. Lollmahomed, F.; Huck, L. A.; Harrington, C. R.; Chitnis, S. S.; Leigh, W. J. *Organometallics* **2009**, *28*, 1484.
3. Huck, L. A.; Leigh, W. J. *Organometallics* **2007**, *26*, 1339.
4. Leigh, W. J.; Potter, G. D.; Huck, L. A.; Bhattacharya, A. *Organometallics* **2008**, *27*, 5948.